

S-Diff: An Anisotropic Diffusion Model for Collaborative Filtering in Spectral Domain

Rui Xia
Nanjing University of Aeronautics
and Astronautics
Nanjing, China
xiarui@nuaa.edu.cn

Yanhua Cheng
Kuaishou Technology
Beijing, China
chengyanhua@kuaishou.com

Yongxiang Tang
Kuaishou Technology
Beijing, China
tangyongxiang@kuaishou.com

Xiaocheng Liu
Kuaishou Technology
Beijing, China
liuxiaocheng@kuaishou.com

Xialong Liu
Kuaishou Technology
Beijing, China
liuxialong2007@sina.com

Lisong Wang
Nanjing University of Aeronautics
and Astronautics
Nanjing, China
wangls@nuaa.edu.cn

Peng Jiang
Kuaishou Technology
Beijing, China
jp2006@139.com

ABSTRACT

Recovering user preferences from user-item interaction matrices is a key challenge in recommender systems. While diffusion models can sample and reconstruct preferences from latent distributions, they often fail to capture similar users' collective preferences effectively. Additionally, latent variables degrade into pure Gaussian noise during the forward process, lowering the signal-to-noise ratio, which in turn degrades performance. To address this, we propose S-Diff, inspired by graph-based collaborative filtering, better to utilize low-frequency components in the graph spectral domain. S-Diff maps user interaction vectors into the spectral domain and parameterizes diffusion noise to align with graph frequency. This anisotropic diffusion retains significant low-frequency components, preserving a high signal-to-noise ratio. S-Diff further employs a conditional denoising network to encode user interactions, recovering true preferences from noisy data. This method achieves strong results across multiple datasets.

CCS CONCEPTS

• **Information systems** → **Recommender systems**; • **Computing methodologies** → **Neural networks**.

KEYWORDS

Diffusion Models, Collaborative Filtering

ACM Reference Format:

Rui Xia, Yanhua Cheng, Yongxiang Tang, Xiaocheng Liu, Xialong Liu, Lisong Wang, and Peng Jiang. 2025. S-Diff: An Anisotropic Diffusion Model for Collaborative Filtering in Spectral Domain. In *Proceedings of the Eighteenth ACM International Conference on Web Search and Data Mining (WSDM '25)*, March 10–14, 2025, Hannover, Germany. ACM, New York, NY, USA, 10 pages. <https://doi.org/10.1145/3701551.3703490>

1 INTRODUCTION

In recent years, generative methods, particularly diffusion models, have gained significant popularity in recommendation systems [22, 42, 49]. These methods capitalize on the potential of complex denoising networks and iterative sampling processes to achieve exceptional performance. By incorporating multimodal learning [20, 28], graph representation learning [17, 28, 52], contrastive learning [4, 26], and negative sampling strategies [27, 30], these models consistently demonstrate valuable advantages across diverse scenarios, establishing them as a highly sought-after approach in the community.

Despite recent advancements, diffusion-based recommendation models still face several challenges. One critical limitation is that traditional diffusion models primarily depend on individual user interaction vectors as conditional inputs, failing to fully utilize the rich shared preference information across users in collaborative filtering, which diminishes the model's capability of interpretation and generalization [16, 48, 52]. Moreover, injecting large amounts of Gaussian noise into high-dimensional historical interaction vectors complicates the recovery process for the denoising decoder [1, 42], a challenge that cannot be overlooked. On the one hand, while some models have attempted to explicitly use collaborative information as conditional guidance for the denoising network (decoder) to improve the quality of recovery [16], the forward process (encoder) does not reflect collaborative signals, which to some extent leads to inconsistency between the encoding and decoding processes. On the other hand, some models [42, 51] encode users' high-dimensional

Permission to make digital or hard copies of all or part of this work for personal or classroom use is granted without fee provided that copies are not made or distributed for profit or commercial advantage and that copies bear this notice and the full citation on the first page. Copyrights for components of this work owned by others than the author(s) must be honored. Abstracting with credit is permitted. To copy otherwise, or republish, to post on servers or to redistribute to lists, requires prior specific permission and/or a fee. Request permissions from permissions@acm.org.

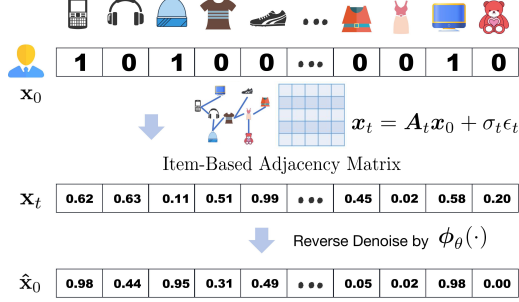
WSDM '25, March 10–14, 2025, Hannover, Germany

© 2025 Copyright held by the owner/author(s). Publication rights licensed to ACM.

ACM ISBN 979-8-4007-1329-3/25/03

<https://doi.org/10.1145/3701551.3703490>

Figure 1: Graph-guided diffusion: By smoothing the interaction signals of users through neighboring item adjacencies, thereby turning them into noise, it is possible to train a denoising network to recover the original signals.



interactions into latent layers using clustering methods to reduce the difficulty of recovering from noise distribution. However, it is still unclear whether these latent representations effectively capture the unique characteristics of collaborative filtering data.

Graph-based collaborative filtering methods [2, 43] offer a promising solution to the first challenge, as they are well-suited to capturing users' shared preferences by iteratively extracting interaction information from low to high orders, leading to notable performance improvements. Notably, graph convolution is often seen as a destructive process, as it can gradually result in the "over-smoothing" of interaction signals. This reminds us of the probability diffusion guided by signal smoothing techniques applied in computer vision, such as image blurring and heat diffusion [37, 45]. These approaches have gone beyond the traditional Gaussian diffusion framework, leading to notable advancements in image and multimedia analysis. Coincidentally, diffusion dynamics on graphs have become increasingly popular in recent years [23, 33], which has also inspired our desire to combine this paradigm with probabilistic diffusion models, enabling user interaction signals to merge with global preferences during the forward destructive phase (see Fig. 1).

It is noteworthy that the success of graph collaborative filtering owes much to advances in graph signal processing, which emphasize the importance of leveraging graph smoothness to retain low-frequency information representing global preferences while filtering out high-frequency noise, thereby progressively smoothing interaction signals across nodes. Building on this, we introduce an anisotropic diffusion model in the item-based graph spectrum domain, where the noise scheduling parameter of the diffusion process is defined by the corresponding graph's eigenvalue coefficients.

Specifically, we correlate the noise scheduling parameters of the diffusion model with the eigenvalue coefficients of the graph spectrum. This approach preserves the low-frequency components during multi-step diffusion. Correspondingly, the reverse denoising process serves as a filter to remove the noise across different frequency components.

Additionally, to mitigate the challenging situation caused by excessive noise from forward diffusion, we propose flexible variance-preserving parameter settings that enhance the modulation of collaborative signals. This allows for a more accurate restoration of user preferences. Specifically, our contribution lies in:

- We introduce a forward diffusion process defined in the graph spectral domain, which effectively incorporates the global preferences of users.
- We propose a parameterized approach to modulating the noise scale of different frequency components, and our analysis and experimental results on signal-to-noise ratio demonstrated the benefits of this setting.
- Correspondingly, in the reverse process, we devise an element-wise fusion-based denoising module, and extensive experiments have validated the efficacy of our proposed method.

In Section 2, we introduce the background of diffusion models for collaborative filtering. In Section 3, we present the method proposed in this paper, transitioning from spatial diffusion models to those in the spectral domain. Section 4 records the results of the experiments, and finally, in Sections 5 and 6, we discuss the existing work and summarize the paper, respectively.

2 BACKGROUND

2.1 Preliminaries

Collaborative filtering can be elegantly framed as an inverse problem, amenable to resolution through the application of generative models. We denote the set of users by \mathcal{U} and the set of items by \mathcal{I} . For every user within \mathcal{U} , in the setting of collaborative filtering with implicit feedback, our dataset is encapsulated by a user-item interaction matrix $X \in \{0, 1\}^{|\mathcal{U}| \times |\mathcal{I}|}$. Each row $x_u \in \{0, 1\}^{|\mathcal{I}|}$ of this matrix represents the interaction vector for user u , where $x_{u,i} = 1$ signifies an interaction between user u and item i , and $x_{u,i} = 0$ indicates the absence of such an interaction. For the sake of simplicity, we will henceforth refer to the user's historical interaction vector as x . Our primary goal is to predict a score vector $\hat{x} \in \mathbb{R}^{|\mathcal{I}|}$, which serves to generate potential preference scores (or probabilities) for all items in \mathcal{I} for a specified user. Subsequently, we aim to recommend the top K items that are most likely to align with and fulfill the user's preferences and needs.

Item-based Graph. The interaction matrix X serves as a bridge, delineating the adjacency relationships between user nodes and item nodes within the context of a user-item bipartite graph. To facilitate the smoothing of interaction vectors, it becomes imperative to quantify the similarity between any two item nodes. To this end, we introduce $D_U = \text{diagMat}(X\mathbf{1})$ and $D_I = \text{diagMat}(X^T\mathbf{1})$, which respectively represent the degree matrices for users and items. Besides, we define the normalized similarity adjacency matrix for item-to-item relationships as $A = \tilde{X}^T \tilde{X}$, where $\tilde{X} = D_U^{-\frac{1}{2}} X D_I^{-\frac{1}{2}}$. This definition enables us to construct the Laplacian operator $L = I - A$, which plays a pivotal role in graph spectral theory and is instrumental in our subsequent analysis and algorithm design.

Graph Fourier Transform (GFT). Moreover, given that the Laplacian matrix L is semi-positive definite and normalized, it can be further decomposed via its eigenvalue decomposition: $L = U^T \Lambda U$. Here, $\Lambda = \text{diag}\{\lambda_1, \dots, \lambda_{|\mathcal{I}|}\}$ is a diagonal matrix composed of the eigenvalues of L , and $U = [u_1, \dots, u_{|\mathcal{I}|}]$ represents a set of corresponding normalized orthogonal eigenvectors. We have the graph Fourier transform (GFT) [38] $v = Ux$, which maps the graph signal x into the graph spectral domain. In this case, each component $v^{(i)}$

of the vector v represents the mapping of the corresponding spatial signal x onto the eigenvalue λ_i .

2.2 Ordinary DDPMs

Representing user interaction vectors as a data distribution that is progressively noised over time steps to become increasingly obfuscated, and then reversing the process to sample and recover from it, forms the basis of generative models [12, 42].

For simplicity, we denote the user’s interaction vector x as x_0 , representing the interaction at the initial time step. Given an initial sample x_0 drawn from the initial user data distribution $q(x_0)$, the forward process of a classical Gaussian diffusion is defined by a sequence of increasingly noisy random variables that deviate from x_0 as,

$$x_t = \alpha_t x_0 + \sigma_t \epsilon_t, \quad \epsilon_t \sim \mathcal{N}(0, I). \quad (1)$$

By setting α_T close to 0, $q(x_T)$ converges to $\mathcal{N}(0, I)$, we are able to sample data x_0 by using a standard Gaussian prior and a learned inference model $p_\theta(x_{t-1} | x_t)$. The inference model p_θ is parameterized as a Gaussian distribution with predicted mean and time-dependent variance scale σ_t^2 , and data can be sampled through sequential denoising, i.e., $p_\theta(x_0) = \prod_{t=1}^T p_\theta(x_{t-1} | x_t)$.

Specifically, we focus on conditional guided diffusion models [7], that is, to recover the true preferences of users through their historical interactions c as a condition. To estimate the conditional distribution $q(x_0 | c)$, the reverse process can be defined as a parameterized hierarchical model:

$$p_\theta(x_{1:T} | x_0, c) = p_\theta(x_T | x_0, c) \prod_{t=1}^T p_\theta(x_{t-1} | x_t, x_0, c), \quad (2)$$

where we set $p(x_T | x_0, c) = \mathcal{N}(x_T; 0, I)$ to guide an ELBO objective function based on c for a conditional diffusion model.

We also set $p_\theta(x_{t-1} | x_t, c) = q(x_{t-1} | x_t, x_0 = \phi_\theta(x_t, c, t))$ for $t = T, \dots, 0$, as well as $p_\theta(x_0 | x_1, c) = \mathcal{N}(x_0; \phi_\theta(x_1, c, 1), \delta^2 I)$, where δ is the variance constant. The remaining task is to learn a neural denoiser ϕ_θ to predict the mean by maximum likelihood estimation.

During the sampling process, we start from random noise $x_T \sim p(x_T)$ and iteratively refine the noise latent variable x_t by sampling $x_{t-1} \sim p_\theta(x_{t-1} | x_t, c)$ for all $t = T, \dots, 0$, ultimately obtaining a final denoised user preference vector \hat{x}_0 .

Notation. To avoid confusion, it is noteworthy that in this paper, the normalized time parameter $t = \tau * t_k / T \in [0, \tau]$ represents a conceptual time step. Here, t_k denotes the actual discrete time steps commonly utilized in diffusion models and τ is a hyper parameter deciding the actual latency of the diffusion process. Besides, the bold font indicates a vector (or matrix), while the non-bold font represents a scalar, such as α and its i -th element, α_i .

3 SPECTRAL DIFFUSION FRAMEWORK IN RECOMMENDATION SYSTEMS

Organization. In Sec. 3.1, we introduce a approach utilizing graph differential equations to guide a forward diffusion process. In Sec. 3.2, we generalize a unified spectral domain diffusion paradigm. Furthermore, we discuss the property and time complexity of the spectral domain diffusion paradigm in Sec. 3.2. In Sec. 3.3, we will outline the procedure for reverse sampling to facilitate recovery, as well as the denoising network employed in the process.

3.1 Graph-Guided Forward Diffusion

We revisit the form of equation (1), inspired by the successes of cold diffusion and diffusion models based on ordinary differential equations (ODEs) across various domains [3, 9, 15, 33, 37, 40, 45]. Indeed, the forward process we construct can be generalized as matrix multiplication followed by additive noise. For instance, in the resolution of image degradation problems, matrix multiplication is instantiated as image blurring or masking to adhere to the prior of real-world problems [35]. When we have precise knowledge about certain properties of the problem to be solved, such a setup can aid in recovery. Inspired by this paradigm, our work slightly deviates from the paradigm of adding noise in scalar form, as seen in equation (1), and instead considers the study of a degradation process in the following form:

$$x_t = C_t x_0 + \sigma_t \epsilon_t, \quad (3)$$

where $C_t : \mathbb{R}^{|\mathcal{I}|} \rightarrow \mathbb{R}^{|\mathcal{I}|}$ is a deterministic linear operator that controls the degeneration in forward-diffusion, and σ_t is the variance constant that controls the level of noise.

As mentioned, we aspire for this degradation operator to align closely with the practices of collaborative filtering tasks. The diffusion of the graph heat kernel [23, 25, 29] guided by the Laplacian matrix L appears promising, as we have chosen the item-item adjacency matrix A . The heat conduction differential equation that unfolds along this matrix implies the smoothing of user interaction signals, which in turn reflects the homophilous preferences of users when clicking items. Specifically, graph heat diffusion introduce a differential equation on the graph, where the greater the difference between two nodes, the faster the derivative smooths it out [23],

$$\frac{dx_i^{(t)}}{dt} = \sum_{j \in \mathcal{N}(i)} A_{ij} (x_j^{(t)} - x_i^{(t)}) = \sum_{j \in \mathcal{N}(i)} A_{ij} x_j^{(t)} - x_i^{(t)}. \quad (4)$$

This equation models the change of the signal $x_i^{(t)}$ at node i over time t . Since the item-item graph’s Laplacian matrix is $L = I - A$, the differential equation of the graph heat diffusion [29] can be stated as:

$$\frac{dx_t}{dt} = -Lx_t, \quad (5)$$

where x_t is the vector of node values at time t , then we proceed to characterize the time decay operator associated with the Laplacian matrix L . Given the initial value x_0 , we have the following when integrating on both sides in Eq. (5)

$$x_t = e^{-Lt} x_0. \quad (6)$$

The diffusion equation can be stated using the $C_t(\cdot)$ satisfied

$$C_t x_0 = e^{-Lt} x_0. \quad (7)$$

Eqs. (6) and (7) show a non-stochastic diffusion process defined by item-item graph. Since the powerful effect of the stochastic diffusion methods such as DDPMs shown in [12, 19], we introduce a Gaussian process $z_t = \sigma_t \epsilon_t$ to serve as noise of our hybrid diffusion process on the graph. Here, scalar sequence σ_t increases monotonically and z_t satisfies $z_{t_2} - z_{t_1} \sim \mathcal{N}(0, (\sigma_{t_2}^2 - \sigma_{t_1}^2)I)$ for any $t_2 > t_1 > 0$, so that $\epsilon_t \sim \mathcal{N}(0, I)$. Now we have the forward process guided by both the diffusion process on the item-item graph and

Figure 2: Spectral Domain Diffusion Models with Anisotropic Noise: We perform an eigenvalue decomposition on the item-based Laplacian matrix, yielding an orthogonal matrix U^T that maps user interaction vectors x into the spectral domain as v , i.e., the Graph Fourier Transform (GFT). We then introduce anisotropic noise into this spectral representation by leveraging the eigenvalues' varying influences. Afterward, we recover the users' original interaction signals from the noisy vector v_T and use the Graph Inverse Fourier Transform (GIFT) to map the decoded signals \hat{v}_0 back to the spatial domain as \hat{x}_u .

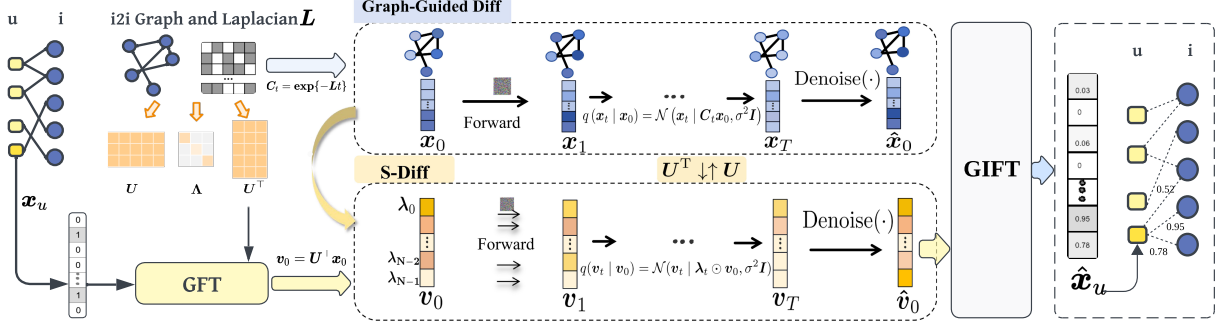
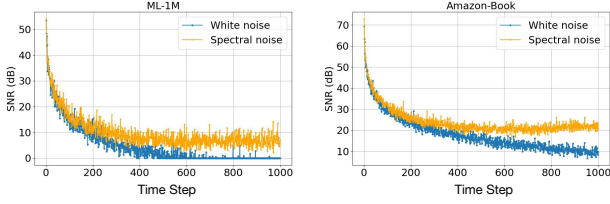


Figure 3: We compare the SNR of the spectral diffusion model across datasets with traditional DDPM using Gaussian noise. Adding eigenvalue-related noise in the spectral domain prevents SNR degradation into white noise.



the stochastic Gaussian process: $x_t = C_t x_0 + \sigma_t \epsilon_t$, which also leads to the distribution of the forward process given by:

$$q(x_t | x_0) = \mathcal{N}(x_t | \mu = C_t x_0, \Sigma = \sigma_t^2 I). \quad (8)$$

3.2 Spectral Diffusion

In this section, we set $(-Lt) = UD_t U^T$, where U^T denotes the orthonormal basis of eigenvectors obtained from matrix decomposition¹, in which D_t is defined by a diagonal matrix whose entries are the eigenvalues arranged as follows: $D_t = \text{diag}\{-td_1, \dots, -td_{|I|}\}$

where $-t \cdot d$ is the corresponding eigenvalue of $-Lt$. According to the definition of the exponential equation for diagonalizable matrices [21], we have $C_t = e^{-Lt} = U \Lambda_t U^T$ satisfied:

$$\Lambda_t = \text{diag}(e^{-t \cdot d_1}, e^{-t \cdot d_2}, \dots, e^{-t \cdot d_{|I|}}).$$

Under the spectral transform $v_t = U^T x_t$, we can express the diffusion process for v_t in the spectral domain as:

$$v_t = \lambda_t \odot v_0 + \sigma_t v_{\epsilon,t} \quad \text{where} \quad v_0 = U^T x_0 \text{ and } v_{\epsilon,t} = U^T \epsilon_t. \quad (9)$$

Here, $v_0 = U^T x_0$ is the frequency response of x_0 , $\lambda_t = [e^{-t \cdot d_1}, e^{-t \cdot d_2}, e^{-t \cdot d_3}, \dots, e^{-t \cdot d_{|I|}}] \in \mathbb{R}^{|I|}$ is the vector formed by the diagonal eigenvalues of D_t , and the Hadamard product is performed element-wise.

¹In practical implementation, we use the Lanczos method to compute the eigenvectors corresponding to the top 200 eigenvalues for the feature space mapping

According to the prior properties of the Gaussian distribution, the frequency domain mapping of Gaussian noise $v_{\epsilon,t}$ in Equation (9) can be re-substituted with a Gaussian noise vector ϵ_t , and we let σ_t be its constant component such that we have noise scale vector $\sigma_t = 1 \cdot \sigma_t$.

Equation (9) indicates that the marginal distribution of frequency v_t decomposes entirely over its scalar elements $v_t^{(i)}$. Similarly, the reverse spectral diffusion model $p_\theta(v_{t-1}|v_t)$ also decomposes entirely. Consequently, we can equivalently describe the scalar form of the diffusion process for each eigenvalue dimension i as follows:

$$q(v_t^{(i)} | v_0^{(i)}) = \mathcal{N}(v_t^{(i)} | \lambda_t^{(i)} v_0^{(i)}, (\sigma_t^{(i)})^2) = \mathcal{N}(v_t^{(i)} | e^{-td_i} v_0^{(i)}, (\sigma_t^{(i)})^2), \quad (10)$$

where $v_t^{(i)} = \lambda_t^{(i)} v_0^{(i)} + \sigma_t \epsilon_t$, with $\epsilon_t \sim \mathcal{N}(0, I)$. This means that performing spatial diffusion guided by the Laplacian matrix can equivalently be defined as a relatively standard Gaussian diffusion process. This diffusion process, defined in the frequency space U , features noise that fluctuates along the amplitude of each eigenvalue, making it anisotropic. Through the equivalence to Gaussian diffusion, we similarly define the spectral diffusion process and the noise scheduling coefficients as follows:

$$q(v_t | v_0) = \mathcal{N}(v | \alpha_t \odot v_0, \sigma_t^2 I). \quad (11)$$

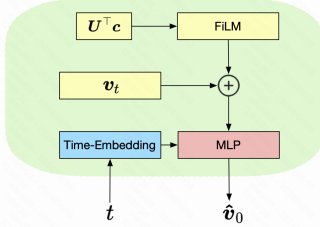
Substituting the choices from [37], we have:

$$\alpha_t = \lambda_t \quad \text{and} \quad \sigma_t^2 = 1 - \lambda_t^2, \quad (12)$$

to construct a variance-preserving diffusion model.

If $\lambda_t^{(i)} = e^{-td_i}$ is chosen such that it maintains lower values at higher frequencies d_i , this is because the negative exponent of e is decreasing. Then $\sigma_t^{(i)}$ will add *more noise* at each time step to the *higher frequency eigenvectors*. Consequently, compared to the diffusion model with standard Gaussian noise, the anisotropic noise introduces noise with specific frequencies (particularly the abnormal high-frequency components) and relatively retains the low-frequency components, which is very similar to the over-smoothing [31, 44] state in graph representation learning.

Boundedness Property. Continuing with the previous notation, where α_t and σ_t represent the noise schedule. For a random variable, the signal-to-noise ratio (SNR) is defined as the ratio of the

Algorithm 1 Training**Require:** $\phi_\theta, \sigma_t, \alpha_t, U, T$ **repeat**Sample u from User Set and let $\mathbf{x}_0 \leftarrow \mathbf{x}_u, \mathbf{c} \leftarrow \text{Mask}(\mathbf{x}_u)$. $\mathbf{v}_0 = U^T \mathbf{x}_0$ Sample $t \sim \mathcal{U}(0, 1)$ and $\mathbf{v}_t \sim \mathcal{N}(\mathbf{v}_t | \alpha_t \odot \mathbf{v}_0, \sigma_t^2 I)$ $\mathbf{c} \leftarrow \emptyset$ with probability $p_{\text{uncond}} = 0.02$ $\hat{\mathbf{v}}_0 = \phi_\theta(\mathbf{v}_t, U^T \mathbf{c}, t)$ Take a gradient step on $\nabla_{\theta} \|\hat{\mathbf{v}}_0 - \mathbf{v}_0\|^2$.**until** convergence**Output:** Denoiser parameters θ .**Figure 4: Instantiation of Denoiser $\phi_\theta(\cdot)$** 

mean squared value to the variance. Given that the mean of \mathbf{v}_0 and \mathbf{v}_t is obviously $\alpha_t \mathbb{E}[\mathbf{v}_0]$, and the variance is σ_t^2 , the SNR is thus $\frac{\alpha_t^2}{\sigma_t^2} \mathbb{E}[\mathbf{v}_0]^2$. Since we are always discussing under the condition of

given \mathbf{v}_0 , we can also simply say that the SNR is $\text{SNR}(t) = \frac{\alpha_t^2}{\sigma_t^2}$, in the commonly used DDPMs, it satisfies $\alpha_0 = \sigma_T = 1, \alpha_T = \sigma_0 = 0$, and in addition, they generally have additional constraints, such as in DDPMs, it is usually $\alpha_t^2 + \sigma_t^2 = 1$. This constraint is also adopted in this paper.

In this case, as t becomes sufficiently large, the SNR will approach zero. This paper state the case of anisotropic diffusion in the spectral domain. Since all eigenvalues $\mathbf{d} = [d_1, d_2, \dots, d_{|I|}]$ of the normalized Laplacian matrix \mathbf{L} are between $[0, 2]$, and $t \in [0, \tau]$, the eigenvalues of \mathbf{C}_t will be within the range $[e^{-2t}, 1]$. This means that we consider: $\text{SNR}(t) = \frac{\alpha_t^2}{\sigma_t^2} = \frac{\alpha_t^2}{1 - \alpha_t^2}$ as the range of this function is greater than $\frac{(e^{-2\tau})^2}{1 - (e^{-2\tau})^2}$, which is to say that the SNR has a good lower bound in S-Diff.

Case Study. As illustrated in Figure 3, under the constraints of bounded anisotropic noise, our spectral domain diffusion process, in contrast to traditional diffusion models, even after 1000 time steps, still retains a discernible signal-to-noise ratio for interaction signals, unlike the complete degeneration into meaningless Gaussian noise observed in traditional models.

Parameter Control. In equation (12), we have established that α_t is related to (λ_t) , forming an anisotropic diffusion paradigm that relies on the eigenvalues of the graph. However, this means that the some eigenvalues may not benefit significantly from the diffusion paradigm. In fact, their recovery may be hindered by high levels of noise. In the case of recommendation data, it is unnecessary to add data to pure noise [1, 46]. Instead, a smaller number of time steps, typically ranging from 3 to 5 steps [42], is used to create a weakly noisy state for recovery. Fortunately, neural diffusion process benefits from the precise parameterization of time step [6, 18].

Algorithm 2 Sampling**Require:** $\phi_\theta, \sigma_t, \alpha_t, U, T, s$ Sample u from User Set and let $\mathbf{c} \leftarrow \mathbf{x}_u$. $\mathbf{v}_0 = U^T \mathbf{c}$ Obtain \mathbf{v}_T via $\mathbf{v}_T = \alpha_T \odot \mathbf{v}_0 + \sigma_T \epsilon_T$ **for** t in $\{\frac{T}{s}, \dots, \frac{1}{s}\}$ **do** $\hat{\mathbf{v}}_0 = (1 - s) \phi_\theta(\mathbf{v}_t, U^T \mathbf{c}, t) + s \phi_\theta(\mathbf{v}_t, 0, t)$ $\epsilon_t \sim \mathcal{N}(0, I)$ $\mathbf{v}_{t-1} \leftarrow \alpha_{t-1} \hat{\mathbf{v}}_0 + \sigma_{t-1} \epsilon_t$ **end for****return** $\hat{\mathbf{x}}_0 = U \hat{\mathbf{v}}_0$

Following the practice in [14], we introduce two hyperparameters, namely α_{\min} and σ_{\max} .

The hyperparameter α_{\min} controls the retention of the minimum frequency. This prevents us from ignoring a sample when its feature value is too small. Additionally, the hyperparameter σ_{\max} controls the maximum noise ratio. It ensures that within the limited number of time steps, the state vector \mathbf{x}_t does not become dominated by pure noise. In summary, by setting appropriate values for α_{\min} and σ_{\max} , we can fine-tune the noise ratio in the diffusion process, which ensures that the diffusion paradigm effectively captures the signal in the data while mitigating the negative impact of noise.

$$\alpha_t = (1 - \alpha_{\min}) \cdot (\lambda_t) + \alpha_{\min}, \quad (13)$$

$$\sigma_t = \text{Min} \left(\sqrt{1 - \lambda_t^2}, \sigma_{\max} \right). \quad (14)$$

Time Complexity. Compared to the regular diffusion model, add spectral diffusion operates under the decomposition dimension \mathbb{R}^K , where K is the approximately truncated dimension, such as the first 200 eigenvalues, utilizing the Lanczos [5] method for matrix decomposition with time complexity of $\mathcal{O}(K|I|m)$, where $|I|$ represents the number of nodes in the item-similarity matrix, $m = 10$ represents the number of iterations in the approximate matrix decomposition process.

3.3 Conditional Reverse and Optimization

Loss function. The loss for a conditional diffusion model is the optimization of a lower bound on the negative log-likelihood of the generated data (ELBO). Specifically, we take the user's initial interaction history as the conditioning vector \mathbf{c} , and step by step, minimizing the KL divergence between the predicted reverse distribution $p_\theta(\mathbf{x}_0 | \mathbf{c})$ and the forward noise distribution $q(\mathbf{x}_{1:T} | \mathbf{c})$ under this condition. We have the decomposed form of the ELBO as:

$$\begin{aligned} \mathcal{L}_{\text{ELBO}} &= \mathbb{E}[-\log p_\theta(\mathbf{x}_0 | \mathbf{c})] \\ &\leq \mathbb{E} \left[-\log \frac{p_\theta(\mathbf{x}_{0:T})}{q(\mathbf{x}_{1:T} | \mathbf{x}_0)} \right] \\ &= \mathbb{E} \left[\sum_{t>1} D_{KL}(q(\mathbf{x}_{t-1} | \mathbf{x}_t, \mathbf{x}_0, \mathbf{c}) \| p_\theta(\mathbf{x}_{t-1} | \mathbf{x}_t, \mathbf{c})) \right] \\ &\quad - \mathbb{E}_{q(\mathbf{x}_1 | \mathbf{x}_0)} [\log p_\theta(\mathbf{x}_0 | \mathbf{x}_1, \mathbf{c})]. \end{aligned} \quad (15)$$

We primarily focus on the general step for sampling and recovery at the intermediate t steps, denoted as \mathcal{L}_t . Specifically, we utilize a neural network $\phi_\theta(\cdot)$, which takes the conditional vector and the noise distribution as inputs, aiming to minimize the discrepancy between the network's output and the user's true interaction vector as the optimization objective. As for the recovery model in the

spectral domain, its optimization objective satisfies:

$$\mathcal{L}_t = \mathbb{E}_{(v_0, v_t) \sim q_0(v_0)q_t(v_t|v_0)} \left[\left\| \left(\phi_\theta(v_t, U^T c, t) - v_0 \right) \right\|^2 \right], \quad (16)$$

where $v_0 = U^T x_0$ and c represents the conditional vector (For example, in a real-world scenario, it is a sequence of past interactions of the user). During the sampling process, we use ϕ_θ for T-step predictions.

Classifier-Free Guidance. To emphasize the effectiveness of the conditional information (user historical interaction information) c , we adopt a classifier-free guidance method [13]. This method simultaneously trains conditional and unconditional diffusion models without the need for classifier guidance on noise signals. Unlike classification-guided techniques, a classifier-free guidance method allows for a balance between sample quality and diversity during inference by adjusting the weighting between conditional and unconditional sampling. Specifically, during training, we maintain a 2% batch dropout for conditional training, i.e., $((\phi_\theta(v_t, 0, t))$.

Instantiation of Denoiser. To ensure consistency with the element-wise anisotropic diffusion in the forward process, we learn the element-wise fusion of the conditional vector and the noise vector during the reverse conditioning recovery using Feature-wise Linear Modulation (FiLM) layer [32]. Specifically, we utilize the FiLM (Feature-wise Linear Modulation) learning functions f and h , which output γ_i and β_i as functions of the element-wise weight of the input $(U^T c)_i$ and the bias term:

$$\gamma_i = f((U^T c)_i), \quad \beta_i = h((U^T c)_i), \quad (17)$$

allowing us to modulate the conditional vector to the noise vector as $v_{fused} = v_t + \gamma \odot (Uc) + \beta$. Then the fused vector together with the sinusoidal time encoding, as inputs to an MLP for denoising, as shown in Fig. (4).

Training. Following the optimization of the objective function, we focus on training the parameters θ within the parameterized denoiser $\phi_\theta(\cdot)$, adhering to the DDPM paradigm in our training and parameterization process. The detailed procedure is outlined as follows:

We initially select user interaction vectors x_0 from the training dataset. Subsequently, a fraction of the interaction history is randomly masked with a 50% probability, serving as the condition c as reported in [42]. The vectors are then transformed into the spectral domain, where noise is added to the initial vector at time step t . The resulting noisy vector, in conjunction with the randomly masked condition c , is fed into the denoising network for denoising. The denoising network $\phi_\theta(\cdot)$ is trained by minimizing the mean squared error (MSE) loss between the generated vector and the clean target vector.

The key idea of this method is described in Algorithm 1 and the output parameters of the denoising network.

Sampling. Once the model is trained, we need a method to generate samples for inference. The simplest idea is to utilize our trained model, $\phi_\theta(v_t, c, t)$, to estimate the noise present in the vector that represents the true interactions. Specifically, whenever we want to move from noise level t to noise level $t - 1$, we can input the noise vector x_t into the model to obtain an estimate of the noise-free

interaction vector, \hat{x}_0 , and then re-add noise to reach level $t - 1$. This idea is summarized in Algorithms 2. It is worth noting that inspired by [52], we use all the historical interactions of users in the test set as the conditional vector c , without masking. We also add noise to this vector to obtain the noisy vector from which we sample to recover.

To collaborate with the Classifier-free training paradigm, we estimate two clear signals, one from a conditional model and the other from an unconditional model, and perform a weighted average of the two signal estimates. The guidance scale (s) is used to regulate the influence of the conditional signal, where a larger scale produces results that are more consistent with the condition, while a smaller scale produces results with less association. We have used an unconditional estimate of $s = 0.02$ for guidance.

4 EXPERIMENT

4.1 Settings

We conducted experiments on three publicly available datasets and used A800s and Tensorflow for training and inference. In this work, we set the batch size to 100, and the learning rate to 1e-4, and do not enable weight decay. We train the model for a maximum of 1,000 epochs. In the temporal dimension, inspired by the successful application of diffusion models in collaborative filtering [42], we set $T = 5$, $\tau = 1$, and t_k is configured as a linearly spaced sequence between $[0, 5]$. Consequently, $t = \tau t_k / T \in [0, 1]$.

Baselines. We compare our model with other widely used collaborative filtering methods.

- ① **MF** [36] is one of the most famous collaborative filtering methods, which optimizes the BPR loss using matrix factorization.
- ② **LightGCN** [10] introduces graph convolutional networks (GCNs) without nonlinear functions into collaborative filtering, iteratively aggregating neighborhood information to learn user and item representations.
- ③ **CDAE** [47] trains an autoencoder (AE) to recover user possible true preferences from degraded vectors.
- ④ **MultiDAE and MultiDAE++** [24] utilizes random masking to break interaction signals and trains the AE to recover this signal.
- ⑤ **MultiVAE** [24] uses variational autoencoders (VAEs) to model the generation process of interaction signals in collaborative filtering and approximates the posterior distribution with an encoder.
- ⑥ **CODIGEM** [41] is the first generative model utilizing diffusion processes, which uses multiple autoencoders to simulate the reverse generation process and uses the predicted vectors for Top-k recommendations.
- ⑦ **DiffRec** [42] refines interaction vectors by mapping them to latent spaces further, and it also proposes weighting the interaction sequences based on timestamps.
- ⑧ **LinkProp**[8] and **BSPM**[2] are examples of graph signal processing techniques applied to collaborative filtering that perform better than embedding-based models on large sparse datasets. BSPM also simulates the sharp process's thermal equation, providing a great inspiration for this work.
- ⑨ **Giff** [52] is a specific case of spatial diffusion, smoothing user signals with graph filters and restoring collaborative signals with corresponding graph denoising operators, achieving outstanding results.

Table 1: Overall performance comparison: We highlight best and second-best values for each metric.

Methods	Amazon-book				Yelp				ML-1M			
	R@10	R@20	N@10	N@20	R@10	R@20	N@10	N@20	R@10	R@20	N@10	N@20
MF	0.0437	0.0689	0.0264	0.0339	0.0341	0.0560	0.0210	0.0276	0.0876	0.1503	0.0749	0.0966
LightGCN	0.0534	0.0822	0.0325	0.0411	0.0540	0.0904	0.0325	0.0436	0.0987	0.1707	0.0833	0.1083
CDAE	0.0538	0.0737	0.0361	0.0422	0.0444	0.0703	0.0280	0.0360	0.0991	0.1705	0.0829	0.1078
MultiDAE	0.0571	0.0855	0.0357	0.0442	0.0522	0.0864	0.0316	0.0419	0.0995	0.1753	0.0803	0.1067
MultiDAE++	0.0580	0.0864	0.0363	0.0448	0.0544	0.0909	0.0328	0.0438	0.1009	0.1771	0.0815	0.1079
MultiVAE	0.0628	0.0935	0.0393	0.0485	0.0567	0.0945	0.0344	0.0458	0.1007	0.1726	0.0825	0.1076
CODIGEM	0.0300	0.0478	0.0192	0.0245	0.0470	0.0775	0.0292	0.0385	0.0972	0.1699	0.0837	0.1087
DiffRec	0.0895	0.1010	0.0451	0.0547	0.0581	0.0960	0.0363	0.0478	0.1058	0.1787	0.0901	0.1148
LinkProp	0.1087	0.1488	0.0709	0.0832	0.0604	0.0980	0.0370	0.0485	0.1039	0.1509	0.0852	0.1031
BSPM	0.1055	0.1435	0.0696	0.0814	0.0630	0.1033	0.0382	0.0505	0.1107	0.1740	0.0838	0.1079
Giff	0.1109	0.1521	0.0733	0.0865	0.0639	0.0992	0.0397	0.0520	0.1108	0.1977	0.0952	0.1176
S-Diff	0.1155	0.1604	0.0746	0.0876	0.0635	0.1075	0.0392	0.0561	0.1277	0.2018	0.0970	0.1225

Table 2: The statistics of three datasets.

Dataset	# of users	# of items	# of interactions	# sparsity
MovieLens-1M	5,949	2,810	571,531	96.6%
Yelp	54,574	34,395	1,402,736	99.93%
Amazon-Book	108,822	94,949	3,146,256	99.97%

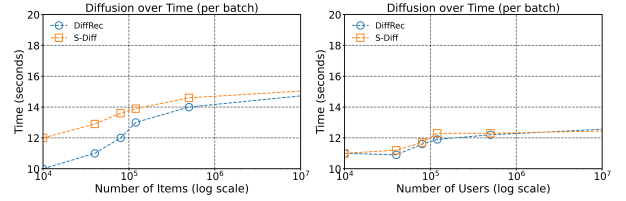
Datasets. To ensure a fair comparison, as shown in Tab. 2, we utilize identical preprocessed and partitioned versions of three public datasets: MovieLens-1M, Yelp, and Amazon-Book, with their respective statistics detailed in Table 2. Each dataset is split into training, validation, and testing subsets in a 7:1:2 ratio. The validation set determines the optimal epoch for each training method, while the testing set is employed for hyperparameter tuning and final result extraction.

In assessing the top-K recommendation efficacy, we present the average Recall@K and NDCG@K. Recall@K gauges the proportion of relevant items recommended within the top-K list, whereas NDCG@K is a ranking-sensitive metric that assigns higher scores to pertinent items positioned higher in the recommendation list.

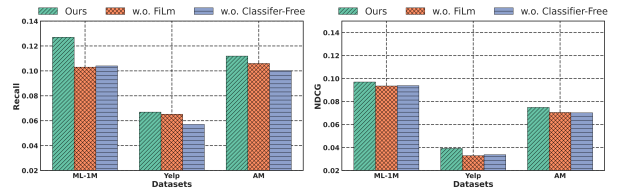
4.2 Performance

Main Results. In Table 1, we recorded the results for Recall and NDCG metrics. All the results were obtained by averaging over 10 runs. The results lead us to the following conclusions:

- ① S-Diff consistently demonstrates significant advantages over all competitors in the recommendation systems, regardless of the dataset or evaluation metrics.
- ② S-Diff exhibits more stable performance compared to other generative models, particularly in metrics like Recall@20, suggesting that anisotropic diffusion on the spectrum effectively preserves users' global preferences, leading to more stable Top-K recommendations.
- ③ The observed improvement across various metrics over previous graph filters indicates that S-Diff's enhanced performance is attributed to the sophisticated multi-step denoising process, which facilitates the optimization of the variational lower bound's robustness, thereby conferring it with robust spectral expressiveness. **Time Cost.** Comparing DiffRec [42], the well-known spatial diffusion paradigm, with the addition of Gaussian noise in the spatial domain and subsequent reverse restoration. In Figure 5, we present the time cost of two diffusion models for inferring a single interaction vector. Following the methodology in [16], we gradually increase the dimension of the collaborative training interaction matrix and record the time taken for one batch of training inference (batch size = 100). Since the diffusion model needs to generate the click

Figure 5: The model's inference time cost for different orders of magnitude of users and items.**Table 3: Frequency-dependent Noise Parameters**

	ML-1M		Yelp	
	R@10	N@10 log(SNR)	R@10	N@10 log(SNR)
DDPM in Spectral	0.0998	0.901	5.25	0.0595 0.0374 7.74
S-Diff-VE	0.1207	0.0942	8.90	0.0610 0.0384 15.89
S-Diff-VP	0.1255	0.0970	12.73	0.0635 0.0392 21.55

Figure 6: We removed the FiLM layer successively, replaced it with concat, and obtained w.o. FiLM, and then used conditional-guidance training to conduct ablation experiments on the denoiser network.

probabilities for all items during the decoding process, it is highly sensitive to the dimensionality of items. As the item dimension increases, the time cost rises significantly. At the same time, the diffusion model is relatively insensitive to the dimensionality of users, even though user nodes are used as stepping stones in the calculation of item-item adjacency matrices. Additionally, S-Diff may initially incur greater costs as it requires additional mapping and remapping, but as the dimensions increase, the time costs converge. Optimizing time costs is also part of future work.

4.3 Ablation

Spectral Parameters. In Tab. 3, we examine the setup in Equation (12), with the aim of understanding the impact of frequency-dependent anisotropic noise on model performance. To this end, we employ the classical DDPM [12] noise schedule in the spectral domain, which we call DDPM in Spectral, where we set α and σ

Figure 7: Sensitivity of the truncated dimension K in matrix decomposition: We examined the impact of the dimension of approximate matrix decomposition on performance across different datasets.

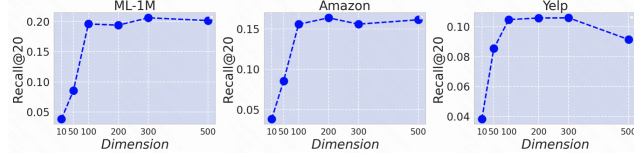
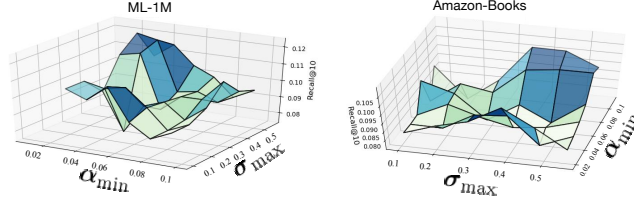


Figure 8: Parameter sensitivity of the bounded noise schedule: We jointly evaluated the impact of the parameters α_{min} and σ_{max} on the recall rate.



as constant factors independent of λ . Given that we configure the square of our diffusion parameters, to sum up to 1 (see Sec. 3.2), adhering to what is known as variance-preserving Diffusion (VP-Diff), we further delve into the effects of the variance-exploding Diffusion (VE-Diff) [39] paradigm in our experiments. Specifically, in VE-Diff, the control of noise σ is no longer constrained by λ and increases uniformly over time steps, as illustrated in the table. The experimental outcomes suggest two key insights:

- 1 The success of the proposed S-Diffusion (S-Diff) paradigm lies in its spectral diffusion approach, which connects with the spectral domain. When employing isotropic diffusion patterns solely in the spectral domain, the performance is akin to that of spatial domain diffusion, highlighting the significance of spectral considerations.
- 2 S-Diff-VP, in comparison to variance exploding Diffusion models, achieves a higher SNR, aligning with our intuition and leading to superior performance. This underscores the importance of a favorable SNR in the recovery of collaborative signals within recommendation tasks, demonstrating that an element-wise controlled noise is crucial for enhancing the precision of collaborative signal restoration.

Denoise Network $\phi_\theta(\cdot)$. In Fig. 6, we conduct ablation experiments on a noise reduction network, successively replacing the FiLM layer with vector concatenation and modifying the training method to classifier guidance to assess the impact of different approaches.

4.4 Sensitivity

Dimension of spectral decomposition. In Fig. 7, we show the influence of spectral decomposition dimension on the performance of the spectral domain diffusion model when it is used for recall. It is worth noting that on the three data sets, we obtain good benefits when we take 200-dimensional spectral decomposition, which is in line with the practice of past researchers.

Boundedness of the diffusion noise schedule. In Fig. 8, we discuss the impact of threshold parameters on the spectral diffusion

model. When we adopt a fixed time step, we impose constraints on the boundedness of α_t and σ_t : the preservation term α_{min} and the noise upper bound σ_{max} . We conduct parameter sensitivity experiments on the MovieLens and Amazon-Book datasets, indicating that a smaller lower bound for feature preservation $\alpha_{min} \in [0, 0.1]$ and a larger upper bound for variance $\sigma_{max} \in [0.4, 0.5]$ contribute to improved performance. Interestingly, on the Amazon-Book dataset, it is necessary to retain smaller eigenvectors for diffusion to achieve the best results.

5 RELATED WORKS

In the introduction, we briefly discussed the related work. Here, we delve deeper into the relevant methods.

On one hand, diffusion models have been employed in recommendation systems [26, 41, 42, 50]. In [41], the DDPMs paradigm was first used in collaborative filtering to recover large-scale interaction matrices. Diffrec [42] improved the accuracy of generative collaborative filtering by using a diffusion model with time-step-guided diffusion and encoding in a latent space. Similarly, methods like DreamRec embed interaction vectors into low-dimensional spaces. It’s worth noting that spectral diffusion models can be seen as a particular case of diffusion in the latent space, reducing the computational complexity of high-dimensional diffusion. The ability of diffusion models for recommendation to capture common user preferences is a question worth considering, as it forms the basis of collaborative filtering’s enduring success [11]. CF-Diff [16, 48] addresses this by pre-computing user’s multi-hop neighborhood information and encoding this information into the conditional of a conditional diffusion model, which may have suboptimal scalability. Giff [52], on the other hand, makes encouraging progress by first breaking down user interaction vectors and then recovering them through graph propagation. Building upon these foundations, we extend the definition of recommendation diffusion models defined on graph spectra, allowing for more flexible parameterization.

Naturally, this anisotropic parameterization process reminds us of the achievements graph filters have made in the past. Among the most notable practices, LightGCN [10] aggregates neighborhood information using multi-layer linear encoding, considered an example of parameter-free graph diffusion. From a spectral theory perspective, it’s often viewed as a low-pass filter. Poly-CF [34] enhances the impact of different frequencies on collaborative filtering by employing adaptive spectral graph filtering. SGFCF [31] additionally demonstrates that collaborative signals at different frequencies contain varying levels of noise, transforming collaborative filtering into a parameterization problem—how to design an adaptive filter to recover the true signal. These works provide crucial theoretical insights, prompting us to experiment by introducing noise at different scales on frequencies corresponding to different eigenvalues and recovering from it.

6 CONCLUSION

In this paper, we introduce a spectral domain diffusion paradigm for collaborative filtering in recommendation systems, which implicitly captures users’ shared preferences. We investigate the theoretical and empirical capabilities of this paradigm, demonstrating its advantages across diverse datasets, and enriching the practice of diffusion models in the recommendation community.

REFERENCES

- [1] Gabriel Bénédict, Olivier Jeunen, Samuele Papa, Samarth Bhargav, Daan Odijk, and Maarten de Rijke. 2023. Recfusion: A binomial diffusion process for 1d data for recommendation. *arXiv preprint arXiv:2306.08947* (2023).
- [2] Jeongwhan Choi, Seoyoung Hong, Noseong Park, and Sung-Bae Cho. 2023. Blurring-sharpening process models for collaborative filtering. In *Proceedings of the 46th International ACM SIGIR Conference on Research and Development in Information Retrieval*. 1096–1106.
- [3] Kaiyuan Cui, Xinyan Wang, Zicheng Zhang, and Weichen Zhao. 2024. Graph Neural Aggregation-diffusion with Metastability. *arXiv preprint arXiv:2403.20221* (2024).
- [4] Ziqiang Cui, Haolun Wu, Bowei He, Ji Cheng, and Chen Ma. 2024. Diffusion-based Contrastive Learning for Sequential Recommendation. *arXiv preprint arXiv:2405.09369* (2024).
- [5] Jane K Cullum and Ralph A Willoughby. 2002. *Lanczos algorithms for large symmetric eigenvalue computations: Vol. I*. Theory. SIAM.
- [6] Giannis Daras, Mauricio Delbracio, Hossein Talebi, Alexandros G Dimakis, and Peyman Milanfar. 2022. Soft diffusion: Score matching for general corruptions. *arXiv preprint arXiv:2209.05442* (2022).
- [7] Anh-Dung Dinh, Daochang Liu, and Chang Xu. 2024. Rethinking conditional diffusion sampling with progressive guidance. *Advances in Neural Information Processing Systems* 36 (2024).
- [8] Hao-Ming Fu, Patrick Poirson, Kwot Sin Lee, and Chen Wang. 2022. Revisiting Neighborhood-based Link Prediction for Collaborative Filtering. In *Companion Proceedings of the Web Conference 2022*. 1009–1018.
- [9] Paul Lyonel Hagemann, Johannes Hertrich, and Gabriele Steidl. 2023. *Generalized normalizing flows via Markov chains*. Cambridge University Press.
- [10] Xiangnan He, Kuan Deng, Xiang Wang, Yan Li, Yongdong Zhang, and Meng Wang. 2020. Lightgcn: Simplifying and powering graph convolution network for recommendation. In *SIGIR*. 639–648.
- [11] Xiangnan He, Lizi Liao, Hanwang Zhang, Liqiang Nie, Xia Hu, and Tat-Seng Chua. 2017. Neural Collaborative Filtering. In *WWW*. ACM, 173–182.
- [12] Jonathan Ho, Ajay Jain, and Pieter Abbeel. 2020. Denoising diffusion probabilistic models. *Advances in Neural Information Processing Systems* 33 (2020), 6840–6851.
- [13] Jonathan Ho and Tim Salimans. 2022. Classifier-free diffusion guidance. *arXiv preprint arXiv:2207.12598* (2022).
- [14] Emiel Hoogeboom and Tim Salimans. 2022. Blurring diffusion models. *arXiv preprint arXiv:2209.05557* (2022).
- [15] Emiel Hoogeboom, Victor Garcia Satorras, Clément Vignac, and Max Welling. 2022. Equivariant diffusion for molecule generation in 3d. In *International Conference on Machine Learning*. PMLR, 8867–8887.
- [16] Yu Hou, Jin-Duk Park, and Won-Yong Shin. 2024. Collaborative Filtering Based on Diffusion Models: Unveiling the Potential of High-Order Connectivity. *arXiv preprint arXiv:2404.14240* (2024).
- [17] Yangqin Jiang, Lianghao Xia, Wei Wei, Da Luo, Kangyi Lin, and Chao Huang. 2024. DiffMM: Multi-Modal Diffusion Model for Recommendation. *arXiv preprint arXiv:2406.11781* (2024).
- [18] Bahjat Kawar, Michael Elad, Stefano Ermon, and Jiaming Song. 2022. Denoising Diffusion Restoration Models. In *Advances in Neural Information Processing Systems*.
- [19] Dongjun Kim, Seungjae Shin, Kyungwoo Song, Wanmo Kang, and Il-Chul Moon. 2022. Soft truncation: A universal training technique of score-based diffusion model for high precision score estimation. In *International Conference on Machine Learning*. PMLR, 11201–11228.
- [20] Zhifeng Kong, Wei Ping, Jiaji Huang, Kexin Zhao, and Bryan Catanzaro. 2021. DiffWave: A Versatile Diffusion Model for Audio Synthesis. In *International Conference on Learning Representations*.
- [21] IE Leonard. 1996. The matrix exponential. *SIAM review* 38, 3 (1996), 507–512.
- [22] Wuchao Li, Rui Huang, Haijun Zhao, Chi Liu, Kai Zheng, Qi Liu, Na Mou, Guorui Zhou, Defu Lian, Yang Song, et al. 2024. DimeRec: A Unified Framework for Enhanced Sequential Recommendation via Generative Diffusion Models. *arXiv preprint arXiv:2408.12153* (2024).
- [23] Yibo Li, Xiao Wang, Hongrui Liu, and Chuan Shi. 2024. A generalized neural diffusion framework on graphs. In *Proceedings of the AAAI Conference on Artificial Intelligence*, Vol. 38. 8707–8715.
- [24] Dawen Liang, Rahul G Krishnan, Matthew D Hoffman, and Tony Jebara. 2018. Variational autoencoders for collaborative filtering. In *WWW*. ACM, 689–698.
- [25] Xixun Lin, Wenxiao Zhang, Fengzhao Shi, Chuan Zhou, Lixin Zou, Xiangyu Zhao, Dawei Yin, Shirui Pan, and Yanan Cao. 2024. Graph Neural Stochastic Diffusion for Estimating Uncertainty in Node Classification. In *Forty-first International Conference on Machine Learning*.
- [26] Qidong Liu, Fan Yan, Xiangyu Zhao, Zhaocheng Du, Huifeng Guo, Ruiming Tang, and Feng Tian. 2023. Diffusion augmentation for sequential recommendation. In *Proceedings of the 32nd ACM International Conference on Information and Knowledge Management*. 1576–1586.
- [27] Shuo Liu, An Zhang, Guoqing Hu, Hong Qian, and Tat-seng Chua. 2024. Preference Diffusion for Recommendation. *arXiv preprint arXiv:2410.13117* (2024).
- [28] Haokai Ma, Yimeng Yang, Lei Meng, Ruobing Xie, and Xiangxu Meng. 2024. Multimodal Conditioned Diffusion Model for Recommendation. In *Companion Proceedings of the ACM on Web Conference 2024*. 1733–1740.
- [29] Jeremy Ma, Weiyu Huang, Santiago Segarra, and Alejandro Ribeiro. 2016. Diffusion filtering of graph signals and its use in recommendation systems. In *2016 IEEE International Conference on Acoustics, Speech and Signal Processing (ICASSP)*. IEEE, 4563–4567.
- [30] Trung-Kien Nguyen and Yuan Fang. 2024. Diffusion-based Negative Sampling on Graphs for Link Prediction. In *Proceedings of the ACM on Web Conference 2024*. 948–958.
- [31] Shaowen Peng, Xin Liu, Kazunari Sugiyama, and Tsunenori Mine. 2024. How Powerful is Graph Filtering for Recommendation. *arXiv preprint arXiv:2406.08827* (2024).
- [32] Ethan Perez, Florian Strub, Harm De Vries, Vincent Dumoulin, and Aaron Courville. 2018. Film: Visual reasoning with a general conditioning layer. In *Proceedings of the AAAI conference on artificial intelligence*, Vol. 32.
- [33] Michael Poli, Stefano Massaroli, Junyoung Park, Atsushi Yamashita, Hajime Asama, and Jinkyoo Park. 2019. Graph neural ordinary differential equations. *arXiv preprint arXiv:1911.07532* (2019).
- [34] Yifang Qin, Wei Ju, Xiao Luo, Yiyang Gu, and Ming Zhang. 2024. PolyCF: Towards the Optimal Spectral Graph Filters for Collaborative Filtering. *arXiv preprint arXiv:2401.12590* (2024).
- [35] Mengwei Ren, Mauricio Delbracio, Hossein Talebi, Guido Gerig, and Peyman Milanfar. 2023. Multiscale structure guided diffusion for image deblurring. In *Proceedings of the IEEE/CVF International Conference on Computer Vision*. 10721–10733.
- [36] Steffen Rendle, Christoph Freudenthaler, Zeno Gantner, and Lars Schmidt-Thieme. 2009. BPR: Bayesian personalized ranking from implicit feedback. In *UAI*. AUAI Press, 452–461.
- [37] Severi Rissanen, Markus Heinonen, and Arno Solin. 2022. Generative modelling with inverse heat dissipation. *arXiv preprint arXiv:2206.13397* (2022).
- [38] Aliaksei Sandryhaila and José MF Moura. 2013. Discrete signal processing on graphs: Graph fourier transform. In *2013 IEEE International Conference on Acoustics, Speech and Signal Processing*. IEEE, 6167–6170.
- [39] Jiaming Song, Chenlin Meng, and Stefano Ermon. 2020. Denoising diffusion implicit models. *arXiv preprint arXiv:2010.02502* (2020).
- [40] Jiaming Song, Arash Vahdat, Morteza Mardani, and Jan Kautz. 2023. Pseudoinverse-guided diffusion models for inverse problems. In *International Conference on Learning Representations*.
- [41] Joojo Walker, Ting Zhong, Fengli Zhang, Qiang Gao, and Fan Zhou. 2022. Recommendation via collaborative diffusion generative model. In *International Conference on Knowledge Science, Engineering and Management*. Springer, 593–605.
- [42] Wenjie Wang, Yiyan Xu, Fuli Feng, Xinyu Lin, Xiangnan He, and Tat-Seng Chua. 2023. Diffusion recommender model. In *Proceedings of the 46th International ACM SIGIR Conference on Research and Development in Information Retrieval*. 832–841.
- [43] Xiang Wang, Xiangnan He, Meng Wang, Fuli Feng, and Tat-Seng Chua. 2019. Neural Graph Collaborative Filtering. In *SIGIR*. ACM, 165–174.
- [44] Yinwei Wei, Xiang Wang, Liqiang Nie, Xiangnan He, Richang Hong, and Tat-Seng Chua. 2019. MMGCN: Multi-modal Graph Convolution Network for Personalized Recommendation of Micro-video. In *MM*. ACM, 1437–1445.
- [45] Jay Whang, Mauricio Delbracio, Hossein Talebi, Chitwan Saharia, Alexandros G Dimakis, and Peyman Milanfar. 2022. Deblurring via stochastic refinement. In *Proceedings of the IEEE/CVF Conference on Computer Vision and Pattern Recognition*. 16293–16303.
- [46] Julia Wolleb, Florentin Bieder, Paul Friedrich, Peter Zhang, Alicia Durrer, and Philippe C Cattin. 2024. Binary Noise for Binary Tasks: Masked Bernoulli Diffusion for Unsupervised Anomaly Detection. *arXiv preprint arXiv:2403.11667* (2024).
- [47] Yao Wu, Christopher DuBois, Alice X Zheng, and Martin Ester. 2016. Collaborative denoising auto-encoders for top-n recommender systems. In *Proceedings of the 9th International Conference on Web Search and Data Mining*. ACM, 153–162.
- [48] Lianghao Xia, Chao Huang, Yong Xu, Huan Xu, Xiang Li, and Weiguo Zhang. 2021. Collaborative reflection-augmented autoencoder network for recommender systems. *ACM Transactions on Information Systems (TOIS)* 40, 1 (2021), 1–22.
- [49] Yiyan Xu, Wenjie Wang, Fuli Feng, Yunshan Ma, Jizhi Zhang, and Xiangnan He. 2024. DiFashion: Towards Personalized Outfit Generation. *arXiv preprint arXiv:2402.17279* (2024).
- [50] Zhengyi Yang, Jiancan Wu, Zhicai Wang, Xiang Wang, Yancheng Yuan, and Xiangnan He. 2024. Generate what you prefer: Reshaping sequential recommendation via guided diffusion. *Advances in Neural Information Processing Systems* 36 (2024).
- [51] Zixuan Yi, Xi Wang, and Iadh Ounis. 2024. A Directional Diffusion Graph Transformer for Recommendation. *arXiv preprint arXiv:2404.03326* (2024).
- [52] Yunqin Zhu, Chao Wang, and Hui Xiong. 2023. Towards graph-aware diffusion modeling for collaborative filtering. *arXiv preprint arXiv:2311.08744* (2023).

A APPENDIX

Table 4: Symbol table.

Symbol	Description
\mathbf{x}_0	Initial interaction vector drawn from user data distribution $q(\mathbf{x}_0)$.
\mathbf{x}_t	Noisy interaction vector at time step t .
α_t	Time-dependent scaling factor.
σ_t	Time-dependent noise scale.
L	Graph Laplacian matrix.
A	Adjacency matrix of the graph.
U	Orthonormal basis of eigenvectors from spectral decomposition of L .
D_t	The diagonal matrix with eigenvalues, $D_t = \text{diag}\{-td_1, \dots, -td_{ I }\}$, satisfies $(-Lt) = UD_tU^T$.
C_t	The forward graph heat diffusion operator, C_t , satisfies $C_t = e^{-Lt} = U\Lambda_tU^T$.
Λ_t	The diagonal matrix obtained from the spectral decomposition of C_t .
λ_t	The eigenvectors formed by different dimensions of Λ_t , also implying the high-frequency and low-frequency information of the graph.
ϵ_t	Gaussian noise, $\epsilon_t \sim \mathcal{N}(\mathbf{0}, I)$.
c	User's historical interaction data.
ϕ_θ	Neural denoiser parameterized by θ .
$\hat{\mathbf{x}}_0$	Final denoised preference vector.
\mathbf{v}_0	Latent spectral vector, $\mathbf{v}_0 = U^T \mathbf{x}_0$.
\mathbf{v}_t	Noisy latent spectral vector at time step t .
s	Strength of unconditional guidance.
p_{uncond}	Probability of unconditional sampling.